Allicin Ameliorates IMQ-induced psoriasis-like Skin Inflammation Via Disturbing the Interaction of Keratinocytes with IL-17A

Lu Zhang[1], Xuehong Ma[1], Rongmei Shi[1], Libo Zhang[2], Ruolin Zhao[2], Ran Duan[2], Yuanyuan Qin[2], Sijia Gao[2], Xinxia Li[1], Jingjing Duan[2], and Jianguang Li[1]

[1]Xin Jiang Medical University
[2]China Pharmaceutical University

May 17, 2022

Abstract

Background and Purpose: Psoriasis is an inflammatory skin disease of chronic recurrence mediated by the interaction between IL-17 and keratinocytes, which sustains a vicious circle of inflammation. Currently, there is no safe and effective natural medicine for the clinical treatment of psoriasis. Given its prominent anti-proliferative and anti-inflammatory properties, we investigated the mechanism of allicin improving psoriasis. Experimental Design: Pharmacodynamics and toxicology experimental studies were estimated after topical administration of allicin on the skin of mice. Changes in inflammatory factors expression were analyzed by qPCR and immunohistochemistry after topical treatment with allicin in mice with psoriasis-like lesions induced by imiquimod. The impacts of allicin on proliferation and apoptosis of keratinocytes were analyzed by CCK8 assay and flow cytometry. The interaction between IL-17A and keratinocytes was studied using HaCaT cells, and the mechanism of action of allicin was explored by Western Blot. Transcriptomic changes following the action of allicin were probed by RNA-seq. Key Results: Our study demonstrated that allicin significantly improved the epidermal structure by inhibiting excessive proliferation and evasion of apoptosis of keratinocytes. Furthermore, allicin reduced the secretion of inflammatory cytokines (IL-17A/F, IL-22, IL-12, IL-20), chemokines (CXCL2, CXCL5, CCL20), and antibacterial peptides (S100A8/9). Mechanistically, allicin directly inhibited the IL-17-induced TRAF6/MAPK/NF-ϰB and STAT3/NF-ϰB signaling cascades in keratinocytes, thus breaking the positive inflammation feedback and alleviating imiquimod-induced psoriasis-like dermatitis in mice. Importantly, topical administration of allicin did not cause skin allergy, and the safety and adaptability of long-term application were verified.

Introduction

Psoriasis is a chronic inflammatory mediated autoimmune skin disease in which keratinocytes and immune cells play central roles. The characteristic histological findings of psoriasis mainly include the aberrant proliferation of keratinocytes and brisk immune cells infiltration. Erythema and scaling appearance of psoriasis lesions severely impact the patient's quality of life. At present, the most advanced therapy currently includes neutralizing antibodies and immunosuppressors for treating psoriasis, which is effective but has many disadvantages, including high cost and systemic side effects such as infection of the upper respiratory tract(Hawkes *et al.* , 2017; Armstrong *et al.* , 2020). Therefore, there remains a need for novel drugs with improved efficacy and less toxicity.

At present, the pathogenesis of psoriasis remains unclear. Many studies have confirmed that the development and maintenance of psoriasis occur through the interplay between inflammatory factors and keratinocytes(Pasquali *et al.* , 2019; Ghoreschi *et al.* , 2021). An increasing body of evidence suggests that IL-17A is a critical inflammatory mediator that mainly targets keratinocytes and drives changes within psoriatic lesions(Martin*et al.* , 2013; Kirkham *et al.* , 2014; Blauvelt *et al.* , 2018). In keratinocytes, IL-17 activates a series of signal transduction factors to induce the production of chemokines (CXCL1, CXCL8, and

CCL20) and other inflammatory factors such as antimicrobial peptides (AMPs, including S100A8, S100A9), which recruit T cells and myeloid dendritic cells to the psoriatic lesions(Blauvelt *et al.* , 2018; Christmann *et al.* , 2020). The positive feedback loop of inflammation in the local skin lesions amplifies and exacerbates the chronic inflammatory process of psoriasis. Although monoclonal antibodies that block IL-17 are effective for psoriasis, the benefits of reducing the interaction between IL-17 and keratinocytes have not been widely studied.

It is widely acknowledged that inflammation response is initiated by multiple signaling pathways, including the mitogen-activated protein kinase (MAPK) and nuclear factor-kB (NF-κB) signaling(Zhao *et al.* , 2021). The critical contribution of the MAPK and NF-κB pathways in psoriasis has been documented in multiple studies(Zhang*et al.* , 2018; Wang *et al.* , 2021). NF-κB is a critical transcription factor of inflammatory genes, which responds to inflammation by binding to specific promoter elements in target genes. Tumor necrosis factor (TNF) receptor-associated factor 6 (TRAF6) has been reported to be a signaling adaptor that can regulate the activation of MAPK and NF-κB(Matsumoto*et al.* , 2018). Ample evidence suggests that IL-17 promotes the expression of inflammatory chemokines and AMPs through NF-κB in keratinocytes(Harper *et al.* , 2009; Wang *et al.* , 2013). IL-17 can also induce the signal transducer and activator of transcription 3 (STAT3) phosphorylation to activate the NF-κB(Kim*et al.* , 2017). Therefore, blocking the IL-17-induced activation of NF-κB is a promising way to alleviate psoriatic dermatitis. The significance of blocking the downstream signal of IL-17 targeting keratinocytes and thus inhibiting the progression of psoriasis warrants further studies.

Natural medicine have become new therapeutic options for the treatment of psoriasis given their good efficacy and few side effects. Garlic is a dietary additive rich in organic sulfur-containing organosulfur compounds, with specific pharmacological properties, such as antioxidant(Zhang *et al.* , 2006), anti-inflammatory(Wang *et al.* , 2017), anti-tumor(Sarvizadeh *et al.* , 2021), immune regulation, and anti-fungal[15](Caporaso *et al.* , 1983). Allicin (diallylthiosulfinate) is the main active ingredient of garlic, rapidly produced from the non-proteinogenic amino acid S-allyl cysteine sulfoxide (alliin) catalyzed by the alliinase enzyme in the presence of water (Borlinghaus *et al.* , 2014; Rose *et al.* , 2019). Given that allicin is not chemically stable and has a short half-life, we extracted stable precursors alliin and alliinase from garlic, which can continuously produce allicin in situ when mixed with an appropriative solvent on the skin tissue. However, the involved mechanism of allicin on anti-inflammatory response in psoriasis has not been documented.

The present study showed that allicin ameliorates imiquimod (IMQ)-induced psoriatic lesions by inhibiting IL-17A expression and abnormal proliferation of keratinocytes. Mechanistically, allicin inhibits IL-17A/IMQ induced NF-κB signaling transcriptional activation and downregulates the expression of chemokines and AMPs in keratinocytes. Our data substantiate the hitherto undocumented therapeutic potential of allicin in alleviating psoriasis.

Materials and methods

Reagents

5% Imiquimod Cream (3 g: 0.15 g, 40201001, Sichuan Med-shine Pharmaceutical), Allicin ointments contains two tubes, tube A loads alliin (1.7, 2.0, 3.4, 4.0, 5.0, 8.0 mg/g,) and alliinase, tube B is the special solvent for tube A loaded water-soluble gel, mixed equal A and B before use (Xinjiang Ailexin Pharmaceutical Co., Ltd). Calcipotriol cream (0.005%, 15 g: 0.75 mg, Chongqing Huapont Pharmaceutical Co., Ltd). Triamcinolone acetonide and econazole cream (10 g: econazole: 0.10 g, triamcinolone acetonide:10 mg, Hunan Dinuo Pharmaceutical Co., Ltd), 1-chloro-2, 4-dinitrobenzene (Tokyo Chemical Industry), Recombinant Human Il-17A (PeproTech, Cat#200-17).

Antibodies

TRAF6 (Cat# 66498-1-Ig), ERK1/2 (Cat# 11257-1-AP), p-ERK1/2 (Thr202/Tyr204) (Cat# 80031-1-RR), JNK (Cat# 24164-1-AP), Phospho-JNK (Tyr185, Cat# 80024-1-RR), STAT3 (Cat# 10253-2-AP), Bax (Cat# 50599-2-lg), Bcl-2 (Cat# 26593-1-AP), Caspase3 (Cat# 19677-1-AP), Ki67 (Cat# 27309-1-AP),

IL-17A (Cat# 26163-1-AP), CD3 (Cat# 17617-1-AP), F4/80 (Cat# 28463-1-AP) were purchased from ProteinTech. Myeloperoxidase (Cat# MPO, ab9535) was purchased from Abcam. P38 (Cat# WL00764) and Phospho-p38(Thr180/Tyr182) (Cat# WLP1576) were purchased from Wanleibio. Phospho-STAT3 (Tyr705, Cat# 9145), NF-κB p65 (Cat# 8242), Phospho-NF-κB p65 (Ser536, Cat# 3033) were purchased from Cell Signaling Technology.

Preparation of Allicin

Allicin is biosynthesized from alliin catalyzed by alliinase extracted from garlic, as previously reported(Li *et al.* , 2011). Alliin (purity [?] 99%, batch No. AL160615) was accurately weighed and dissolved in DMEM medium to make the stock solutions (1.0 mg/mL). Alliinase ([?]10000U/g, batch No. 201801001) was freshly prepared and dissolved at 37 to ensure optimal enzyme activity. Equal volumes were mixed for 30min at room temperature to ensure that alliin sufficiently reacted with alliinase. Centrifuged for 10 minutes at 4 °C at 12,000 rpm, the allicin stock solution was diluted immediately prior to experimentation. The allicin and alliinase were provided by Xinjiang Ailexin Pharmaceutical Co., Ltd (Xinjiang, China).

Cell Culture

The human immortalized epidermal keratinocyte cell line HaCaT was purchased from the iCell Bioscience Inc (Shanghai, China, passages 20–22) and maintained in high-glucose Dulbecco's Modified Eagle Medium (DMEM, BIOIND, Israel) contained 10% fetal bovine serum (FBS, BIOIND, Israel) and 1% penicillin-streptomycin (PS, NCM Biotech, China) under standard conditions (37°C with 95% humidity and 5% CO_2). Cells were digested by 0.25% trypsin-EDTA and terminated by DMEM containing 10% FBS.

Cell Viability Assay

The cell viability was determined by Cell Counting Kit-8 (CCK8) according to the manufacturer's protocol (Cat#C0043, Beyotime, China). HaCaT cells (1×104 cells/200μl) were seeded into 96-well plates overnight and incubated with different concentrations of allicin for 48 h. After adding 20μl of CCK-8 solution to each well for 1 h at 37°C, the optical density (OD) was measured using a multifunctional microplate reader (2300, PerkinElmerEnSpire) at 450 nm.

Treatment of Psoriasis-like Skin in Mice

A total of eight groups of BALB/c mice (male and female, 8-11 weeks, 20-25 g) were randomly selected (n = 6 per group) and purchased from Vital River Laboratory Animal Technology Co., Ltd. (Beijing, China), containing normal control group (NC), IMQ group, vehicle control group, allicin-low-dose group (AL, 1.7 mg/g, measured with alliin), allicin-middle-dose group (AM, 3.4 mg/g, measured with alliin) and allicin-high-dose group (AH, 5.0 mg/g, measured with alliin), positive control groups, with the commonly used first-line treatment for psoriasis, calcipotriol cream (15 g: 0.75 mg) or triamcinolone acetonide and econazole cream (TAE). 5cm^2 of the back skin of mice was exposed by shaving dorsal hair. A daily topical dose of 62.5 mg IMQ for inducing psoriasis-like skin was provided at 9:00 a.m. for six consecutive days. Then mice were treated with allicin ointment twice, at an interval of four hours. Vehicle control mice were topically treated with a blank allicin-free gel. The experiment was terminated on the seventh day, following sacrifice of the mice, the back skin was dissected rapidly and flash frozen in liquid nitrogen and stored at 80°C for subsequent analyses.

Measurement of Skin Inflammation Severity

We used the cumulative Psoriasis Area and Severity Index (PASI) score to assess the severity of skin lesions, which consists of erythema, scale, and thickness. The score was graded independently from 0 to 4: 0, none; 1, slight; 2, moderate; 3, marked; 4, very marked. The PASI scores of the mice were recorded on the first day of IMQ treatment.

Skin Sensitization Test

Guinea pigs (both sexes, 6-7 weeks, 330-410 g) were purchased from Pizhou Orient Breeding (Jiangsu, China)

and randomly assigned into three groups (n=10). The back hair was removed before the skin sensitization test. The Control group was treated with a blank solvent, and the allicin-treated group received topical allicin treatment (4 mg/g, measured with alliin). In the positive control group, 1-chloro-2, 4-dinitrobenzene (WT6CA-VO, Tokyo Chemical Industry) was used as a contact-sensitizing agent; a 1% sensitization concentration solution or 0.1% excitation concentration was prepared with ethanol. On sensitization day, guinea pigs were treated on the left skin, and on the excitation day were treated on the right skin. The first sensitization and administration day was defined as the first day of the test (D1). Guinea pigs were sensitized on Days 1, 8 and 15), and all groups were stimulated 14 days after the last sensitization (D29). The allergic reactions of the skin were observed at 6 h, 24 h, 48 h, and 72 h. Skin anaphylaxis includes erythema and edema. The evaluation criteria of erythema: without erythema (0), barely visible erythema (1), visible erythema (2), severe erythema (3), purplish-red erythema with mild eschar (4); The evaluation criteria of edema: without edema (0), barely visible edema (1), obviously higher than the edge of the surrounding skin (2), skin bulge 1mm or clear contour (3), skin bulge more than 1mm or blisters or ulceration (4).

Toxicity Assay of Repeated Administration and Skin Irritation Test

New Zealand rabbits (both sexes, 14-16 weeks, 2.3-2.7 kg) were purchased from Qindao Kangda Biological Technology (Shandong, China), randomly assigned into four groups (n=10) contained control-group (blank solvent), allicin low-dose group (2 mg/g, measured with alliin), allicin middle-dose group (4 mg/g, measured with alliin), and allicin high-dose group (8 mg/g, measured with alliin). After four consecutive months of topical administration of allicin, body weight, organ weight, hematologic and clinical chemistry analysis were evaluated. Skin irritation included erythema and edema and was evaluated based on the above criteria. Stimulus Scores = Total Cumulative Stimulus Scores / Total Observation Times. Stimulation grade: without irritation (0-0.49), mild irritation (0.5-2.99), moderate irritation (3.0-5.99), severe irritation (6.0-8.00).

Hematoxylin and Eosin Staining

Collected back skin tissues from mice were conserved in 10% formaldehyde solution for 72 h, then dehydrated. Hematoxylin and eosin (H&E) staining was performed on 4 mm thick paraffin-embedded sections. The tissue sections were examined under an OLYMPUS light microscope. Histological scores were evaluated by a cumulative score containing four independent scoring criteria (0-4): Epidermal thickness, inflammatory cells infiltrate, capillaries dilatation, and parakeratosis. Three different fields of view were used to measure the thickness of the mice's epidermis.

Immunohistochemistry

Paraffin sections were deparaffinized with xylene and rehydrated in decreasing ethanol concentrations; then, antigen retrieval was carried out with the EDTA buffer (PH 9.0) for 25 min at 100°C. To neutralize the endogenous peroxidase, sections were cooled down to room temperature and incubated with 3% H_2O_2 for 10 min to neutralize the endogenous peroxidase. After washing twice with PBST (1× PBS with 0.05% Tween 20), sections were blocked with 10% goat serum for 45 min and incubated in the specific primary antibodies against Ki67, IL-17A, CD3, F4/80, and myeloperoxidase (MPO) with appropriately diluted ratio overnight at 4°C. After washing with PBST, tissues were incubated with HRP-conjugated goat anti-rabbit secondary antibody for 45 min at room temperature. All sections were stained using DAB for a few seconds and lightly counterstained with hematoxylin. Images were obtained with an Olympus BX41 microscope.

TUNEL staining

The apoptosis cells in the skin lesions of mice were detected using the One Step TUNEL Apoptosis Assay Kit (C1086, Beyotime). After deparaffinization and rehydration, skin slices were treated with proteinase K (20 μg/ml) for 20 min at 37 and then rinsed in PBS three times. According to the manufacturer's instructions, sections were stained with TUNEL staining reagents at 37°C for 60 min. Following several washes with PBS, nuclei were stained with DAPI Staining Solution (C1005, Beyotime) for 3 min at room temperature. Images were obtained using an inverted fluorescence microscope (Leica, DMI3000B), in which TUNEL-positive cells produced green fluorescence, and DAPI yielded blue fluorescence.

Western Blotting Analysis

Total protein was extracted from snap-frozen skin tissues or HaCaT cells using RIPA buffer (P0013J, Beyotime) containing 1% phosphatase and protease inhibitors. After centrifugation, clarified lysates were quantified using the BCA Protein Assay Kit (Thermo Scientific) and boiled with SDS loading buffer at 95 for 15 min. Then, we separated protein samples by sodium dodecyl sulfate-polyacrylamide gel electrophoresis (SDS-PAGE) and transferred them to polyvinylidene fluoride (PVDF) membranes (Amersham International), where 5% milk in TBST (TBS with 0.05% Tween 20) was used as the blocking buffer to block the membrane at room temperature for 1 h. Next, primary antibodies were diluted to a suitable concentration based on the manufacturer's recommendations by dilution buffer (P0023A, Beyotime) and incubated overnight at 4 degC. After three washes in TBST, the protein samples were incubated with horseradish peroxidase (HRP)-conjugated secondary antibodies at room temperature for 2 h. The protein bands were detected by the enhanced chemiluminescence (ECL) western-blotting substrate (Fdbio science, FD8000) and quantified using Image Lab (Bio-Rad).

Reverse Transcription and Real-time PCR Analysis

Total RNA was extracted from snap-frozen skin tissues or HaCaT cells using the Trizol Reagent (Thermo Fisher Scientific, 15596026) on ice in an RNAse free environment, after which complementary DNAs were synthesized using the HiScript III 1st Strand cDNA Synthesis Kit (+gDNA wiper) (Vazyme Biotech, R312-01). The qRT-PCR was performed using the Step One Plus Real-Time PCR system (Applied Biosystems). β-Actin was used as the reference gene for normalization. The fold changes of mRNA relative expression were calculated using the comparative cycle method (2-ΔΔCt). The primer sequences are shown in Supplementary Table S1.

Cell cycle analysis

HaCaT cells were seeded in six-well plates and allowed to adhere. Then the cells were serum-starved for 24 h, followed by treatment with 10%-FBS/DMEM containing various concentrations of allicin (6.4, 9.6, 12.8μg/mL) for 48 h. Later, the cells were collected by trypsinization and fixed in 70% ethanol overnight at -20°C. After being washed with PBS, HaCaT cells were resuspended and incubated with PI/RNase staining buffer according to the manufacturer's instructions (C1052, Beyotime) for 30 min at 37°C in the dark and then subjected to flow cytometric analysis. The samples were acquired with the Attune NxT (Thermo Fisher Science), and the cell cycle distribution was further analyzed using ModFit software (Verity Software House).

Cell apoptosis assay

Annexin V-FITC Apoptosis Detection Kit (Beyotime, China) was used to quantitatively evaluate allicin-induced apoptosis. The supernatant was collected and mixed with HaCaT cells detached using EDTA-free trypsin. After centrifugation, HaCaT cells were resuspended in PBS. Then cells were incubated with 195μl binding buffer and incubated with 5μl Alexa Fluor 488 and 10μl PI for 15 min at room temperature. The proportion of cell apoptosis was measured by flow cytometry and analyzed with FlowJo V10.

RNA-seq analysis

Total RNA was extracted from the back skin lesions of the IMQ-treated and high-dose allicin-treated groups for transcriptome sequencing. RNA was isolated and purified using Trizol reagent (Invitrogen, Carlsbad, CA, USA). The RNA amount and purity of each sample were quantified using NanoDrop ND-1000 (Wilmington, DE, USA). The final cDNA was sent for library preparation and sequencing on an Illumina Novaseq 6000 at LC Bio Technology (Hangzhou, China). With StringTie and Ballgown, we estimate the expression levels for all transcripts and calculate the expression levels for mRNAs with FPKM (FPKM = [total exon fragments/mapped reads (millions) × exon length (kB)]). The differentially expressed genes (DEGs) were selected by R package edgeR or DESeq2 with fold change > 2 or fold change < 0.5 and p-value < 0.05. Following that, we conducted gene ontology (GO) enrichment and Kyoto encyclopedia of genes and genomes (KEGG) enrichment analyses of the differentially expressed mRNAs in the two groups.

Statistical analysis

All data are presented as mean ± SEM (standard error of the mean). GraphPad Prism was used to compare two groups using Unpaired Student's t-tests and one-way ANOVA followed by Tukey's post hoc test for comparing multiple groups using one-way ANOVA (Version 8.0.1), and statistically significant differences are indicated as follows: *p < 0.05, **p < 0.01, ***p < 0.001, ****p < 0.0001.

Results

Allicin Ameliorated IMQ-Induced Psoriasis-like Skin Lesion in Mice

IMQ-treated mice skin exhibited typical psoriatic characteristics, such as acanthosis, inflammatory cell infiltrates, and altered dermal vascularity. Therefore, IMQ was applied to mouse skin to explore how allicin interferes with the pathophysiology of psoriasis. To assess allicin's effect on restoring the appearance of psoriatic lesions induced by IMQ, we consecutively applied IMQ for six days after shaving the back of mice. The treatment groups received mixed ointment with different allicin contents four and eight hours after receiving IMQ (Figure 1A). Compared with the normal control group, IMQ treatment exhibited apparent erythema and scaling of the skin, whereas the phenotypic changes in allicin-treated groups were significantly improved (Figure 1B). Dorsal skin thickness, erythema and scaling were scored daily from 0-4 according to the severity degree. Additionally, an overall evaluation of skin lesions was depicted by a modified PASI score (0-12), calculated by summing the three individual scores. Compared with the IMQ-group, allicin-treated groups showed a significant alleviation in erythema severity (Figure 1C), scaling (Figure 1D), and thickening (Figure 1E). Figure 1F showed a better overall improvement with allicin treatment than positive control groups. H&E staining showed that the epidermal layer of the IMQ-treated group was significantly incrassated, and the corium layer was infiltrated by inflammatory cells accompanied by vascular hyperplasia. However, the characteristic pathological changes of the skin in the allicin-treated groups were significantly improved compared with the model group (Figure 1G, H). These results collectively indicated that allicin was efficient in relieving IMQ-induced psoriasis-like lesions.

Preclinical Safety Evaluation of Allicin on Topical Application

Further evaluation of skin irritability and irritation induced by allicin was performed to assess the suitability and safety of allicin for topical applications. Skin changes were observed after allicin treatment daily, including erythema and edema. As shown in Figures 2A and 2B, no allergic reactions were observed in the allicin administration group. After four months of continuous application, compared with the blank solvent control group, allicin led to slight skin irritation in the first three months and yielded no irritation in the fourth month due to gradual development of skin tolerance (figure 2C). Next, we inspected the toxicity of allicin for long-term application, and there was no significant influence on weight (Figure 2D). The organ index was calculated after the major organs were resected and weighed, using the formula Organ index = organ weight (mg) / body weight (kg) ×100%. The heart, liver, spleen, and thymus indexes showed that allicin yielded no significant difference in body weight and major organs compared with the control group (Figure 2E). Hematology (Figure 2F, Table S2) and biochemistry (Table S3) indicators were analyzed before and after continuous topical application of allicin, with no significant changes. Our data demonstrated that allicin was safe and well-tolerated for long-term external use.

Allicin Inhibits Keratinocytes Proliferation in HaCaT and psoriatic lesions

Sustained abnormal proliferation is the hallmark of keratinocytes in psoriatic lesions; thus, we investigated whether allicin inhibits the proliferation of keratinocytes in IMQ-induced psoriatic skin. HaCaT cells were treated with different concentrations of allicin (3.2, 6.4, 9.6, 12.8, 25.6, 51.2 μg/mL), and the cell viability was assessed by CCK8 assays after 48h (figure 3A). The effect of allicin treatment was concentration-dependent and significantly reduced cell viability. We next analyzed the influence of allicin on the cell distribution in the different cell cycle phases with flow cytometry. Allicin significantly decreased the HaCaT cell numbers in the G0/G1 phase, whereas the number of cells in the G2/M phase was increased compared with the control group (Figure 3B). The percentage of cells in the G2/M increased from 21.62% to 58.33%, indicating that

allicin inhibited the proliferation of keratinocytes by inducing G2/M cell cycle arrest (Figure 3C). We used immunohistochemistry analysis to examine the expression of Ki67 in skin lesions, which is a marker expressed in proliferating cells. Figure 3D showed that the Ki67 expression of allicin-treatment was significantly fewer than with the IMQ-treated group. These results demonstrate that allicin reduced epidermal thickness by inhibiting keratinocyte hyperproliferation.

Allicin Induces Keratinocytes Apoptosis in vivo and vitro

The resistance of keratinocytes to apoptosis is well-established to contribute to psoriatic epidermal thickening. We examined the effect of allicin on inducing apoptosis in keratinocytes. An analysis of flow cytometry with Annexin V/PI staining was carried out to determine the percentage of apoptotic cells. As shown in Figures 4A and 4B, the proportion of apoptotic cells was 8.74%, 21.90%, and 29.40% after treatment with 6.4, 9.6, and 12.8μg/mL of allicin, respectively, which was significantly higher than the control group (5.39%). Overall, treatment with various concentrations of allicin dose-dependently induced keratinocyte apoptosis. The molecular mechanism of allicin-mediated apoptosis was explored using Western blot. Allicin induced the levels of pro-apoptotic proteins Bax and cleaved-caspase3 and inhibited the expression of the anti-apoptotic protein Bcl-2 in HaCaT cells (Figures 4C) and skin lesions (Figures 4D). In addition, TUNEL-DAPI staining was performed to examine keratinocyte apoptosis in skin lesions sections. Figure 4E showed that allicin treatment could induce keratinocyte apoptosis in psoriatic skin. These data corroborated the pro-apoptotic role of allicin in keratinocytes of psoriasis skin lesions.

Identification of IL-17 as a Key Target Regulated by Allicin through RNA-seq

To further uncover the molecular mechanism of underlying disruption of IMQ-induced psoriasis development by allicin, we used RNA-sequencing (RNA-seq) to compare gene alternations between IMQ-treated and allicin-treated groups. A Volcano plot depicting changes in differentially expressed genes (DEGs) after Allicin treatment is shown in Figure 5A. Compared with the IMQ-treated group, 1285 genes were significantly altered, including 344 downregulated and 941 upregulated genes in the allicin-treated group (fold change[?]2 and $q<0.05$). Among these DEGs, the downregulated genes were closely associated with inflammation (Figure 5B). KEGG analysis showed that the DEGs were involved in various signaling pathways, including cytokine-cytokine receptor interaction, basal cell carcinoma, Wnt signaling pathway, and IL-17 signaling pathway (Figure 5C). The gene expression level of IL-17A and IL-17F was significantly different, which further confirmed that allicin could alleviate IMQ-induced psoriasis-like skin inflammation in mice through the IL-17-mediated signaling pathway. GO enrichment analysis indicated that the downregulated DEGs were mainly enriched in biological processes associated with signal transduction and innate immune response (Figure 5D). Taken together, these results indicated IL-17-associated inflammatory genes and IL-17 signal pathways were regulatory targets of allicin in IMQ-induced psoriasis-like inflammatory skin.

Allicin Reduced the Secretion of Inflammatory Factors and Immune Cells Infiltration in IMQ-Induced Mouse Model

Psoriasis and other inflammatory skin diseases are widely thought to result from abnormal cytokine expression. IL-17 mediates inflammatory cell recruitment via inducing inflammatory cytokines and chemokines by keratinocytes in psoriatic lesions(Nograles *et al.* , 2008; Harper *et al.* , 2009). We examined the mRNA expression levels of inflammatory cytokines in IMQ-induced psoriasis skin lesions. As seen in Figures 6A and 6C, allicin significantly suppressed the mRNA levels of IL-17A. Then the expression of IL-17A was further validated by IHC (Figure 6C). In addition, allicin reduced IL-12, IL-20, and IL-22 levels, which are involved in the immune response of psoriasis (Figure 6B). Various immune cell subsets create a self-sustaining cycle of inflammation during the development of psoriasis, including T cells, neutrophils, and macrophages(Singh *et al.* , 2013). Current evidence suggests that the number of $CD3^+$cells is increased in the skin tissue of patients with psoriasis (He *et al.* , 2021). We next determined whether allicin affected the accumulation of immune cells in IMQ-induced psoriasis-like skin, including T cells, macrophages, and neutrophils. The immunohistochemistry results showed that allicin reduced the infiltration of $CD3^+$, $F4/80^+$, and MPO^+ cells compared to the IMQ-treated group (Figure 6D, E, F). As a result, allicin treatment alleviated immune

cell infiltration and pro-inflammatory factor secretion substantially.

Allicin Reduced the mRNA Expression of Chemokines and Antimicrobial Peptides (AMPs) both in IMQ-induced psoriatic lesions and IL-17A Stimulated HaCaT Cells

IL-17A is a potent stimulator of multiple immune-related proteins such as chemokines and AMPs, which lead to further inflammatory responses in keratinocytes of psoriasis lesions(Furue*et al.* , 2020). Excessive expression of AMPs in psoriatic lesions is involved in the pathogenesis of dermatoses via host inflammatory reactions, such as cathelicidin, β-defensins, and S100 proteins(Wang *et al.* , 2018). To investigate whether allicin could reduce the production of chemokines and AMPs by keratinocytes upon IL-17A stimulation, we measured the mRNA expression of CXCL8, CCL20, S100A8, and S100A9 by RT-qPCR. The data showed IL-17A remarkedly upregulated levels of CXCL8, CCL20, S100A8, and S100A9, which were notably reduced in the allicin-treated group (Figure 7A). Similarly, compared with the IMQ-group, allicin significantly decreased the mRNA expression levels of CXCL2, CXCL5, CCL20, S100A8, and S100A9 in psoriasis-like lesions (Figure 7B).

Αλλιςιν Ινηιβιτεδ ΙΛ-17Α-αςτιατεδ ΤΡΑΦ6/ΜΑΠΚ ανδ ΣΤΑΤ3/ΝΦ-κΒ Σιγναλινγ Πατηωαψς ιν ϊτρο ανδ ιν ϊο

It has been confirmed that activated IL-17A signaling recruits TRAF6, which leads to simultaneous activation of the NF-κB by MAPK phosphorylation(Kobayashi *et al.* , 2003). Topical application of IMQ induces IL-17-mediated psoriatic dermatitis via TRAF6 signaling. In addition, IL-17-enhanced NF-κB transcriptional activity in keratinocytes was stimulated by the activation of STAT3 and NF-κB pathways. We next co-cultured keratinocytes with IL-17A with or without allicin, then further detected the activation of TRAF6, ERK1/2, P38, JNK, STAT3, and P65. Figure 8A showed that IL-17A stimulation for 30 min effectively upregulated the phosphorylation expression of ERK1/2, P38, JNK, and P65 in HaCaT cells, while treatment with allicin significantly inhibited the protein expression of TRAF6 and MAPK and restrained the phosphorylation of MAPK, STAT3, and P65 (Figure 8B, 8C). To investigate whether allicin alleviates IMQ-induced psoriatic lesions by inhibiting downstream pathways activated by IL-17A, we analyzed the protein expressions of TRAF6/MAPK/STAT3/NF-κB, which were significantly repressed in IMQ-induced psoriatic lesions (Figure 8D, 8E). Overall, the results showed that allicin could inhibit inflammation by suppressing the activation of IL-17A downstream signaling pathways (Figure 8F).

Discussion

The dynamic interplay between keratinocytes and T cell-derived cytokines is crucial in the initiation and maintenance phases of psoriatic alterations, perpetuating inflammation in a vicious cycle(Jiang *et al.* , 2020). Keratinocytes play multiple roles in psoriatic skin lesions as the target cell of IL-17 and the producer of cytokines, leading to the infiltration of inflammatory cells. More importantly, keratinocytes are the main initiator of pathological changes in psoriatic skin due to uncontrolled proliferation and differentiation. Our study demonstrates that blocking the feedback between keratinocytes and inflammatory factors is a promising approach for treating psoriasis.

Although traditional treatment therapies are effective, psoriasis is not cured and is often recurrent, emphasizing the importance of long-term safe and effective drugs. Accordingly, nontoxic, widely accessible, and inexpensive natural products have gained momentum as a novel strategy in recent years. Diallyl trisulfide, a sulfur compound found in garlic, has been developed and approved to treat fungal and bacterial infections. The anti-inflammatory, antiviral, and anticancer properties of allicin prompt us to explore its potential in psoriasis. Based on our in vitro and in vivo results, allicin alleviates psoriasis by suppressing inflammation and hyperproliferation. Indeed, the influence of the topical application of allicin on the systemic immune system was negligible compared to systemic administration. Our data identified that allicin treatment did not induce significant changes in body weight and immune organ index values, indicating that allicin treatment was safe, with no significant side effects on mice. The present study substantiates that allicin is a promising natural drug candidate for psoriasis.

We used the first-line drugs corticosteroids (TAE) and topical vitamin D corticosteroid (calcitriol) in the present study as positive control drugs. We demonstrated that allicin treatment has therapeutic effects on inflammation comparable to the positive groups; moreover, improvement of erythema and scales showed higher therapeutic efficacy with allicin than with positive drugs. This finding may be attributed to the fact that current first-line drugs merely inhibit inflammation and suppress proliferation and differentiation of keratinocytes, while the anti-psoriasis effect of allicin is multifaceted. Our results showed that allicin not only decreased IL-17 secretion but also triggered inhibition of keratinocyte viability and cell cycle progression and promoted apoptosis, which directly relieved epidermal swelling.

Keratinocytes are actively involved in the pathogenesis and maintenance of psoriasis by producing various pro-inflammatory factors and chemokines. S100A8/9 and CCL20 are additional factors during IL-17-driven dermal inflammation, which are strongly induced preferentially during the early maturation of keratinocytes(Christmann *et al.* , 2020; Elnabawi *et al.* , 2021). Overwhelming evidence substantiates that S100A8/9 and CCL20 are overexpressed in human psoriatic lesions, whereas serum concentrations of S100A8/S100A9 and CCL20 are reliable biomarkers for monitoring disease activity in psoriasis, including psoriatic arthritis or infections, underlining their clinical relevance(Benoit *et al.* , 2006; Schonthaler *et al.* , 2013; Austermann *et al.* , 2017; Dey *et al.* , 2017; Freise *et al.* , 2019). Consistent with previous reports, we identified upregulated expression of IL-17-dependent CCL20 and S100a8/9, both in HaCaT cells and in mice psoriatic skin lesions. Our study corroborated that allicin inhibited immune cell infiltration in skin lesions; however, we did not investigate the effect of allicin on systemic immune cells in depth. Mechanistically, allicin inhibited transcription of NF-$\varkappa$B induced by IL-17, which triggered the expression of psoriasis-relevant target genes encoding for CCL20 and S100A8/9. Overall, our data suggest that interfering with IL-17 signaling in keratinocytes is a promising strategy for treating psoriasis. Targeting the IL-17 signaling pathway may improve treatment response and prevent treatment resistance.

Interestingly, it has been reported that allicin inhibits the activation of the MAPK/NF-$\varkappa$B pathway and NLRP3 inflammasome to improve acrylamide-induced hepatotoxicity(Li *et al.* , 2020). Furthermore, allicin alleviated reticuloendotheliosis virus infection-induced inflammation and oxidative damage by blocking the ERK/MAPK pathway(Wang *et al.* , 2017). In addition, alliin ameliorated gut inflammation by suppressing MAPKs-PPAR-γ/NF-$\varkappa$B/AP-1/STAT-1 signaling pathways(Shi *et al.* , 2017). These studies corroborated that allicin yields superior anti-inflammatory effects by regulating MAPKs and NF-$\varkappa$B. During the transcriptome analysis of allicin-treated and IMQ-treated mice lesions, we observed dramatic changes in IL-17-dependent genes expression following IL-17A/F gene expression down-graduation, and substantial enrichment in IL-17 signaling pathways, confirming the in vivo molecular mechanisms of allicin are related to IL-17 signaling in psoriasis. Hyperactivity of the IL-17 signaling pathway in psoriatic lesions further exacerbates the inflammatory response. Importantly, the inhibition of IL-17 and IL-17 signaling blocks various signaling pathways in keratinocytes. In this study, we documented the pivotal role of allicin in blocking the IL-17 signaling pathway, including TRAF6, MAPKs (ERK1/2, P38, JNK), STAT3, and NF-$\varkappa$B (P65).

Conclusion

This study elucidated the molecular mechanism of allicin in improving IMQ-induced psoriatic lesions in mice. In this regard, allicin inhibits the innate immune response to external stimuli in psoriatic lesions, resulting in reduced expression of pro-inflammatory cytokines and chemokines. Furthermore, allicin treatment mitigates psoriasis progression by inhibiting the TRAF6/MAPK/NF-$\varkappa$B and STAT3/NF-$\varkappa$B signaling pathways and activating the apoptotic signaling cascade in keratinocytes. Overall, our data substantiated that interfering with IL-17 signaling in keratinocytes with allicin is a promising strategy for treating psoriasis, given its safety and effectiveness.

Ethics statement:

The animal study was reviewed and approved by the Institutional Animal Care and Use Committee of the Center for New Drug Safety Evaluation and Research, China Pharmaceutical University.

Declaration of transparency and scientific rigor

According to the BJP guidelines for Design and Analysis, this report adheres to the principles for transparent reporting and scientific rigor of preclinical research.

Conflict of interest statement:

The authors state no conflict of interest.

Funding

This work was supported by the Science Fund for Distinguished Young Scholars of Xinjiang Autonomous Region (No. 2022D01E17) and the Natural Science Foundation of Xinjiang Uygur Autonomous Region (No. 2021D01C255), Major science and technology special project of Xinjiang Uygur Autonomous Region: research and development of the active ingredient of medicinal garlic for external use against difficult skin diseases in Xinjiang.

Authors contribution

Jianguang Li, Jingjing Duan, and Xinxia Li conceived and designed the project. Lu Zhang, Libo Zhang, Ruolin Zhao, Ran Duan, Yuanyuan Qin, Sijia Gao participated in the experiments. Xuehong Ma and Rongmei Shi contributed to the preparation and the quality control of reagent (allicin). Lu Zhang analyzed data and drafted the article. Jingjing Duan edited and reviewed it. Jianguang Li and Xinxia Li critically read the manuscript and gave helpful suggestions. All authors read and approved the final manuscript.

References

[1] J. E. Hawkes, T. C. Chan and J. G. Krueger: Psoriasis pathogenesis and the development of novel targeted immune therapies. J Allergy Clin Immunol, 140(3) (2017) 645-653, doi:10.1016/j.jaci.2017.07.004.

[2] A. W. Armstrong and C. Read: Pathophysiology, Clinical Presentation, and Treatment of Psoriasis: A Review. Jama, 323 (19) (2020) 1945-1960, doi:10.1001/jama.2020.4006.

[3] K. Ghoreschi, A. Balato, C. Enerbäck and R. Sabat: Therapeutics targeting the IL-23 and IL-17 pathway in psoriasis. Lancet, 397 (10275) (2021) 754-766, doi:10.1016/s0140-6736(21)00184-7.

[4] L. Pasquali, A. Srivastava, F. Meisgen, K. Das Mahapatra, P. Xia, N. Xu Landén, A. Pivarcsi and E. Sonkoly: The Keratinocyte Transcriptome in Psoriasis: Pathways Related to Immune Responses, Cell Cycle and Keratinization. Acta Derm Venereol, 99 (2) (2019) 196-205, doi:10.2340/00015555-3066.

[5] B. W. Kirkham, A. Kavanaugh and K. Reich: Interleukin-17A: a unique pathway in immune-mediated diseases: psoriasis, psoriatic arthritis and rheumatoid arthritis. Immunology, 141 (2) (2014) 133-42, doi:10.1111/imm.12142.

[6] A. Blauvelt and A. Chiricozzi: The Immunologic Role of IL-17 in Psoriasis and Psoriatic Arthritis Pathogenesis. Clin Rev Allergy Immunol, 55 (3) (2018) 379-390, doi:10.1007/s12016-018-8702-3.

[7] D. A. Martin, J. E. Towne, G. Kricorian, P. Klekotka, J. E. Gudjonsson, J. G. Krueger and C. B. Russell: The emerging role of IL-17 in the pathogenesis of psoriasis: preclinical and clinical findings. J Invest Dermatol, 133 (1) (2013) 17-26, doi:10.1038/jid.2012.194.

[8] C. Christmann, S. Zenker, L. Martens, J. Hübner, K. Loser, T. Vogl and J. Roth: Interleukin 17 Promotes Expression of Alarmins S100A8 and S100A9 During the Inflammatory Response of Keratinocytes. Front Immunol, 11, (2020) 599947, doi:10.3389/fimmu.2020.599947.

[9] H. Zhao, L. Wu, G. Yan, Y. Chen, M. Zhou, Y. Wu and Y. Li: Inflammation and tumor progression: signaling pathways and targeted intervention. Signal Transduct Target Ther, 6 (1) (2021) 263, doi:10.1038/s41392-021-00658-5.

[10] Z. Wang, H. Zhou, H. Zheng and X. Zhou: Autophagy-based unconventional secretion of HMGB1 by keratinocytes plays a pivotal role in psoriatic skin inflammation, 17 (2) (2021) 529-552, doi:10.1080/15548627.2020.1725381.

[11] C. Zhang, C. Xiao, E. Dang, J. Cao, Z. Zhu, M. Fu, X. Yao, Y. Liu, B. Jin, G. Wang and W. Li: CD100-Plexin-B2 Promotes the Inflammation in Psoriasis by Activating NF-ϰB and the Inflammasome in Keratinocytes. J Invest Dermatol, 138 (2) (2018) 375-383, doi:10.1016/j.jid.2017.09.005.

[12] R. Matsumoto, T. Dainichi, S. Tsuchiya, T. Nomura, A. Kitoh, M. S. Hayden, K. J. Ishii, M. Tanaka, T. Honda, G. Egawa, A. Otsuka, S. Nakajima, K. Sakurai, Y. Nakano, T. Kobayashi, Y. Sugimoto and K. Kabashima: Epithelial TRAF6 drives IL-17-mediated psoriatic inflammation. JCI Insight, 3 (15) (2018) e121175, doi:10.1172/jci.insight.121175.

[13] E. G. Harper, C. Guo, H. Rizzo, J. V. Lillis, S. E. Kurtz, I. Skorcheva, D. Purdy, E. Fitch, M. Iordanov and A. Blauvelt: Th17 cytokines stimulate CCL20 expression in keratinocytes in vitro and in vivo: implications for psoriasis pathogenesis. J Invest Dermatol, 129 (9) (2009) 2175-83, doi:10.1038/jid.2009.65.

[14] C. Q. F. Wang, Y. T. Akalu, M. Suarez-Farinas, J. Gonzalez, H. Mitsui, M. A. Lowes, S. J. Orlow, P. Manga and J. G. Krueger: IL-17 and TNF synergistically modulate cytokine expression while suppressing melanogenesis: potential relevance to psoriasis. J Invest Dermatol, 133 (12) (2013) 2741-2752, doi:10.1038/jid.2013.237.

[15] J. Kim and J. G. Krueger: Highly Effective New Treatments for Psoriasis Target the IL-23/Type 17 T Cell Autoimmune Axis. Annu Rev Med, 68 (2017) 255-269, doi:10.1146/annurev-med-042915-103905.

[16] Z. M. Zhang, N. Zhong, H. Q. Gao, S. Z. Zhang, Y. Wei, H. Xin, X. Mei, H. S. Hou, X. Y. Lin and Q. Shi: Inducing apoptosis and upregulation of Bax and Fas ligand expression by allicin in hepatocellular carcinoma in Balb/c nude mice. Chin Med J (Engl), 119 (5) (2006) 422-425, 10.1001/jama.295.10.1172.

[17] L. Wang, H. Jiao, J. Zhao, X. Wang, S. Sun and H. Lin: Allicin Alleviates Reticuloendotheliosis Virus-Induced Immunosuppression via ERK/Mitogen-Activated Protein Kinase Pathway in Specific Pathogen-Free Chickens. Front Immunol, 8 (2017) 1856, doi:10.3389/fimmu.2017.01856.

[18] M. Sarvizadeh, O. Hasanpour, Z. Naderi Ghale-Noie, S. Mollazadeh, M. Rezaei, H. Pourghadamyari, M. Masoud Khooy, M. Aschner, H. Khan, N. Rezaei, L. Shojaie and H. Mirzaei: Allicin and Digestive System Cancers: From Chemical Structure to Its Therapeutic Opportunities. Front Oncol, 11 (2021) 650256, doi:10.3389/fonc.2021.650256.

[19] N. Caporaso, S. M. Smith and R. H. Eng: Antifungal activity in human urine and serum after ingestion of garlic (Allium sativum). Antimicrob Agents Chemother, 23 (5) (1983) 700-2, doi:10.1128/aac.23.5.700.

[20] J. Borlinghaus, F. Albrecht, M. C. Gruhlke, I. D. Nwachukwu and A. J. Slusarenko: Allicin: chemistry and biological properties. Molecules, 19 (8) (2014) 12591-618, doi:10.3390/molecules190812591.

[21] P. Rose, P. K. Moore, M. Whiteman and Y. Z. Zhu: An Appraisal of Developments in Allium Sulfur Chemistry: Expanding the Pharmacopeia of Garlic. Molecules, 24(21) (2019) 4006, doi:10.3390/molecules24214006.

[22] X. Li and J. Chen: Method for preparing of Allicin injection and low-temperature continuous stirring ultrafiltration device thereof, United States Patent, 2015 US, 9023623B2.

[23] K. E. Nograles, L. C. Zaba, E. Guttman-Yassky, J. Fuentes-Duculan, M. Suárez-Fariñas, I. Cardinale, A. Khatcherian, J. Gonzalez, K. C. Pierson, T. R. White, C. Pensabene, I. Coats, I. Novitskaya, M. A. Lowes and J. G. Krueger: Th17 cytokines interleukin (IL)-17 and IL-22 modulate distinct inflammatory and keratinocyte-response pathways. Br J Dermatol, 159 (5) (2008) 1092-102, doi:10.1111/j.1365-2133.2008.08769.x.

[24] T. P. Singh, C. H. Lee and J. M. Farber: Chemokine receptors in psoriasis. Expert Opin Ther Targets, 17 (12) (2013) 1405-22, doi:10.1517/14728222.2013.838220.

[25] H. He, R. Bissonnette, J. Wu, A. Diaz, E. Saint-Cyr Proulx, C. Maari, C. Jack, M. Louis, Y. Estrada, J. G. Krueger, N. Zhang, A. B. Pavel and E. Guttman-Yassky: Tape strips detect distinct immune

and barrier profiles in atopic dermatitis and psoriasis. J Allergy Clin Immunol, 147 (1) (2021) 199-212, doi:10.1016/j.jaci.2020.05.048.

[26] M. Furue, K. Furue, G. Tsuji and T. Nakahara: Interleukin-17A and Keratinocytes in Psoriasis. Int J Mol Sci, 21 (4) (2020) 1275, doi:10.3390/ijms21041275.

[27] S. Wang, R. Song, Z. Wang, Z. Jing, S. Wang and J. Ma: S100A8/A9 in Inflammation. Front Immunol, 9 (2018) 1298, doi:10.3389/fimmu.2018.01298.

[28] T. Kobayashi, P. T. Walsh, M. C. Walsh, K. M. Speirs, E. Chiffoleau, C. G. King, W. W. Hancock, J. H. Caamano, C. A. Hunter, P. Scott, L. A. Turka and Y. Choi: TRAF6 is a critical factor for dendritic cell maturation and development. Immunity, 19(3) (2003)353-63, doi:10.1016/s1074-7613(03)00230-9.

[29] Y. Jiang, L. C. Tsoi, A. C. Billi, N. L. Ward, P. W. Harms, C. Zeng, E. Maverakis, J. M. Kahlenberg and J. E. Gudjonsson: Cytokinocytes: the diverse contribution of keratinocytes to immune responses in skin. JCI Insight, 5(20) (2020) e142067, doi:10.1172/jci.insight.142067.

[30] Y. A. Elnabawi, M. S. Garshick, M. Tawil, T. J. Barrett, E. A. Fisher, K. Lo Sicco, A. L. Neimann, J. U. Scher, J. Krueger and J. S. Berger: CCL20 in psoriasis: A potential biomarker of disease severity, inflammation, and impaired vascular health. J Am Acad Dermatol, 84 (4) (2021) 913-920, doi:10.1016/j.jaad.2020.10.094.

[31] J. Austermann, S. Zenker and J. Roth: S100-alarmins: potential therapeutic targets for arthritis. Expert Opin Ther Targets, 21 (7) (2017)739-751, doi:10.1080/14728222.2017.1330411.

[32] H. B. Schonthaler, J. Guinea-Viniegra, S. K. Wculek, I. Ruppen, P. Ximénez-Embún, A. Guío-Carrión, R. Navarro, N. Hogg, K. Ashman and E. F. Wagner: S100A8-S100A9 protein complex mediates psoriasis by regulating the expression of complement factor C3. Immunity, 39 (6) (2013) 1171-81, doi:10.1016/j.immuni.2013.11.011.

[33] S. Benoit, A. Toksoy, M. Ahlmann, M. Schmidt, C. Sunderkötter, D. Foell, M. Pasparakis, J. Roth and M. Goebeler: Elevated serum levels of calcium-binding S100 proteins A8 and A9 reflect disease activity and abnormal differentiation of keratinocytes in psoriasis. Br J Dermatol, 155 (1) (2006) 62-6, doi:10.1111/j.1365-2133.2006.07198.x.

[34] N. Freise, A. Burghard and T. Ortkras: Signaling mechanisms inducing hyporesponsiveness of phagocytes during systemic inflammation, 134 (2) (2019) 134-146, doi:10.1182/blood.2019000320.

[35] A. K. Dey, A. A. Joshi, A. Chaturvedi, J. B. Lerman, T. M. Aberra, J. A. Rodante, H. L. Teague, C. L. Harrington, J. P. Rivers, J. H. Chung, M. T. Kabbany, B. Natarajan, J. I. Silverman, Q. Ng, G. E. Sanda, A. V. Sorokin, Y. Baumer, E. Gerson, R. B. Prussick, A. Ehrlich, L. J. Green, B. N. Lockshin, M. A. Ahlman, M. P. Playford, J. M. Gelfand and N. N. Mehta: Association Between Skin and Aortic Vascular Inflammation in Patients With Psoriasis: A Case-Cohort Study Using Positron Emission Tomography/Computed Tomography. JAMA Cardiology, 2 (9) (2017) 1013-1018, doi:10.1001/jamacardio.2017.1213.

[36] C. L. Li, X. H. Liu, Y. Qiao, L. N. Ning, W. J. Li, Y. S. Sun, D. S. Liu, W. Gao and C. M. Ma: Allicin alleviates inflammation of diabetic macroangiopathy via the Nrf2 and NF-kB pathway. Eur J Pharmacol, 876 (2020) 173052, doi:10.1016/j.ejphar.2020.173052.

[37] L. Shi, Q. Lin, X. Li, Y. Nie, S. Sun, X. Deng, L. Wang, J. Lu, Y. Tang and F. Luo: Alliin, a garlic organosulfur compound, ameliorates gut inflammation through MAPK-NF-ϰB/AP-1/STAT-1 inactivation and PPAR-γ activation. Mol Nutr Food Res, 61 (9) (2017) doi:10.1002/mnfr.201601013.

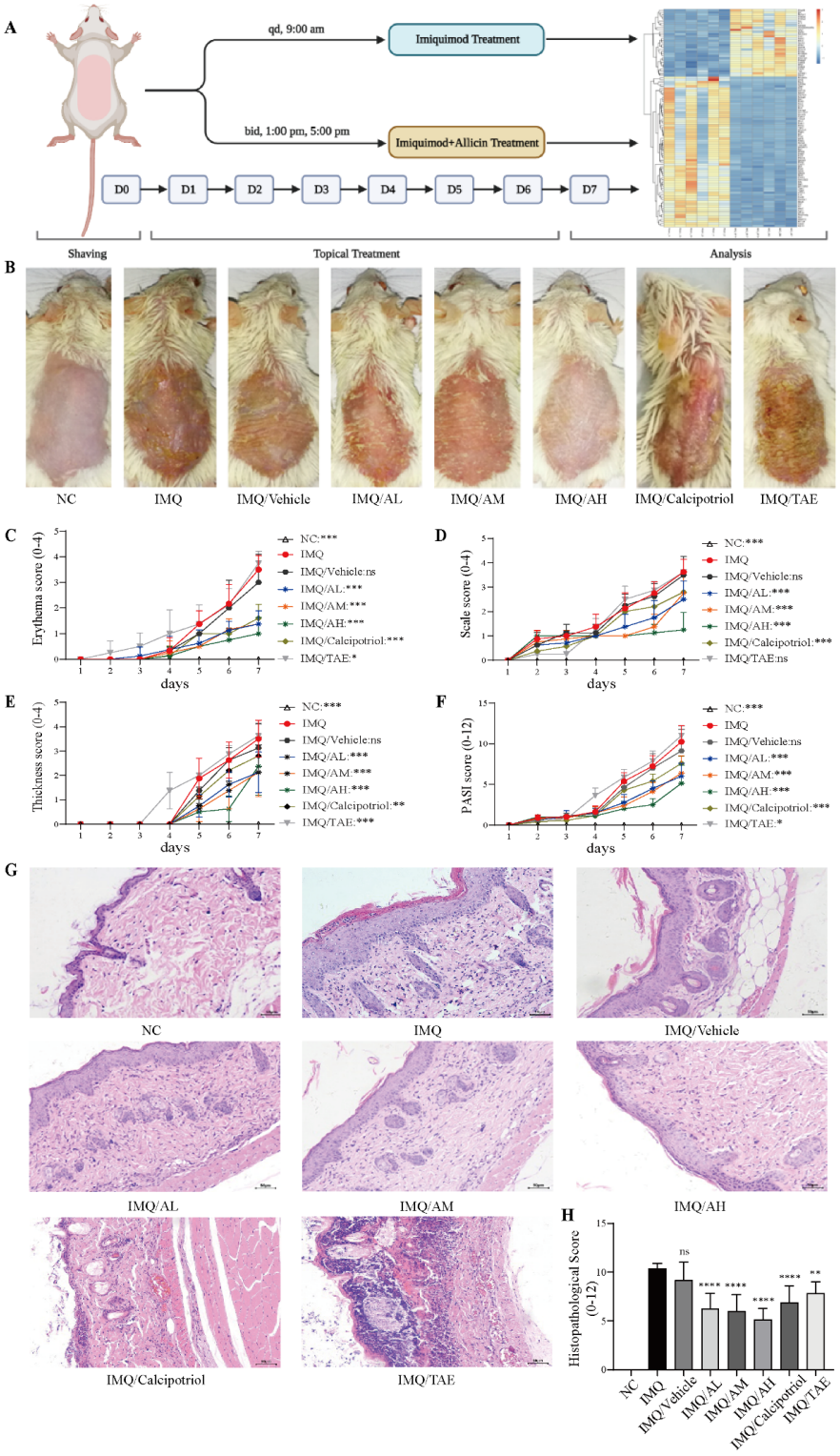

Figure1. Allicin attenuates symptoms of IMQ-induced psoriasis-like lesions in mice. (A) Treatment scheme in the IMQ-induced mice model. (B) Representative images of IMQ-induced psoriatic symptoms on mice

dorsal skin treated with or without allicin for 6 days (AL, allicin low-dose; AM, allicin middle-dose; AH, allicin high-dose; TAE, triamcinolone acetonide and econazole cream). The severity of the IMQ-induced dorsal lesions was evaluated by PASI scores (n=6), and the cumulative scores of redness (C), scale (D), and thickness (E) were measured daily (F). Representative images of H&E staining (G) and respective histopathological scores (H) of IMQ-induced psoriatic lesions in each group (n=3). Scale bar = 50 μm. Data are expressed as means ± SD. *p < 0.05, **p < 0.01, ***p < 0.001, ****p < 0.0001.

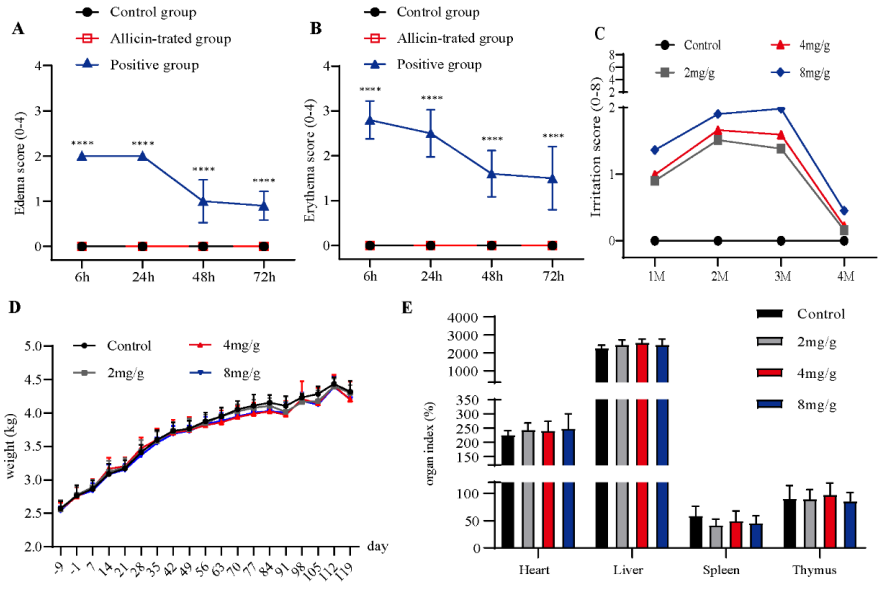

F

Parameter	Time	0mg/kg		2mg/kg		4mg/kg		8mg/kg	
		Male	Famale	Male	Famale	Male	Famale	Male	Famale
WBC(10^9/L)	D(-3)	8.00±1.55	7.76±1.33	8.27±2.36	8.37±0.95	8.26±1.87	8.80±1.51	11.04±4.91	7.51±1.12
	D92	8.08±0.35	11.07±3.88	7.63±1.55	8.55±1.50	7.84±0.43	11.22±3.74	7.67±0.29	7.59±0.82
RBC(10^12/L)	D(-3)	6.23±0.42	5.94±0.34	6.55±0.44	6.18±0.58	6.47±0.75	6.06±0.16	7.23±0.81	5.91±0.65
	D92	6.51±0.52	6.56±0.24	6.14±0.19	6.64±0.64	6.38±0.13	6.29±0.72	6.46±0.45	6.04±0.31
MCV(fL)	D(-3)	64.90±1.50	68.40±3.20	65.50±2.1	67.80±3.80	67.60±1.70	68.00±2.10	67.00±0.7	69.00±2.80
	D92	67.00±2.70	64.70±2.00	65.80±1.8	67.40±3.70	67.00±1.50	64.90±1.30	67.60±1.6	68.50±1.80
PLT(10^9/L)	D(-3)	377±178	466±27	454±184	452±44	355±106	424±54	399±107	379±37
	D92	299±86	404±87	296±102	373±128	293±121	350±61	396±33	305±15
NEU(%)	D(-3)	27.30±5.70	25.50±7.00	33.60±9.50	26.20±5.50	31.30±5.90	21.90±3.90	33.00±16.20	21.10±3.50
	D92	14.70±2.50	25.00±9.00	25.30±5.40	22.00±8.80	20.50±5.00	23.40±10.00	22.00±3.90	20.80±3.50

Abbreviations: WBC, white blood cell; RBC, red blood cell; MCV, mean corpuscular volume; PLT, platelets; NEU, neutrophiles.

Figure2. Safety and adaptability evaluation of allicin topical application on guinea pig and rabbit skin. Edema (A) and erythema (B) scores were recorded at 6h, 24h, 48h, and 72h during the stimulation phase of the anaphylaxis test (n=12). (C) Cumulative scores of skin irritation after allicin topical application with different concentrations in rabbits for 4 months. Effects on body weight (D) and major organ index (E) of different concentrations of allicin applied to rabbit skin for 4 months. (F) Hematologic studies before 3 days and after 92 days of allicin topical administration (n=6). Data are expressed as means ± SD. *p < 0.05, **p < 0.01, ***p < 0.001, ****p < 0.0001.

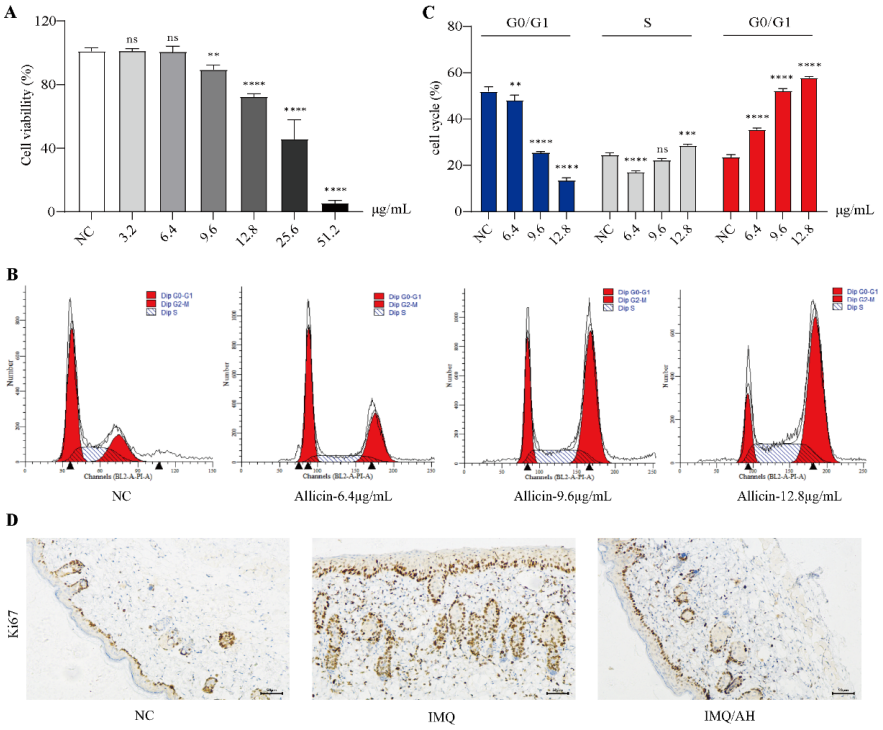

Figure 3. Allicin inhibits hyperproliferation in the keratinocytes. (A) Cell viability of IL-17A-stimulated HaCaT cells treated with different concentrations of allicin was measured by CCK-8 assay (n=6). (B) The cell cycle distribution of PI labeling in different phases with different concentrations of allicin after 48h. (C) Percentages of G0/G1, S, and G2/M-phase cells with different concentrations of allicin after 48h (n=3). (D) Representative immunohistochemical images and the relative expression of Ki67 in IMQ-induced psoriasis-like lesions treated with or without allicin (AH, allicin high-dose). Scale bar = 50 μm. Data are expressed as means ± SD. *p < 0.05, **p < 0.01, ***p < 0.001, ****p < 0.0001.

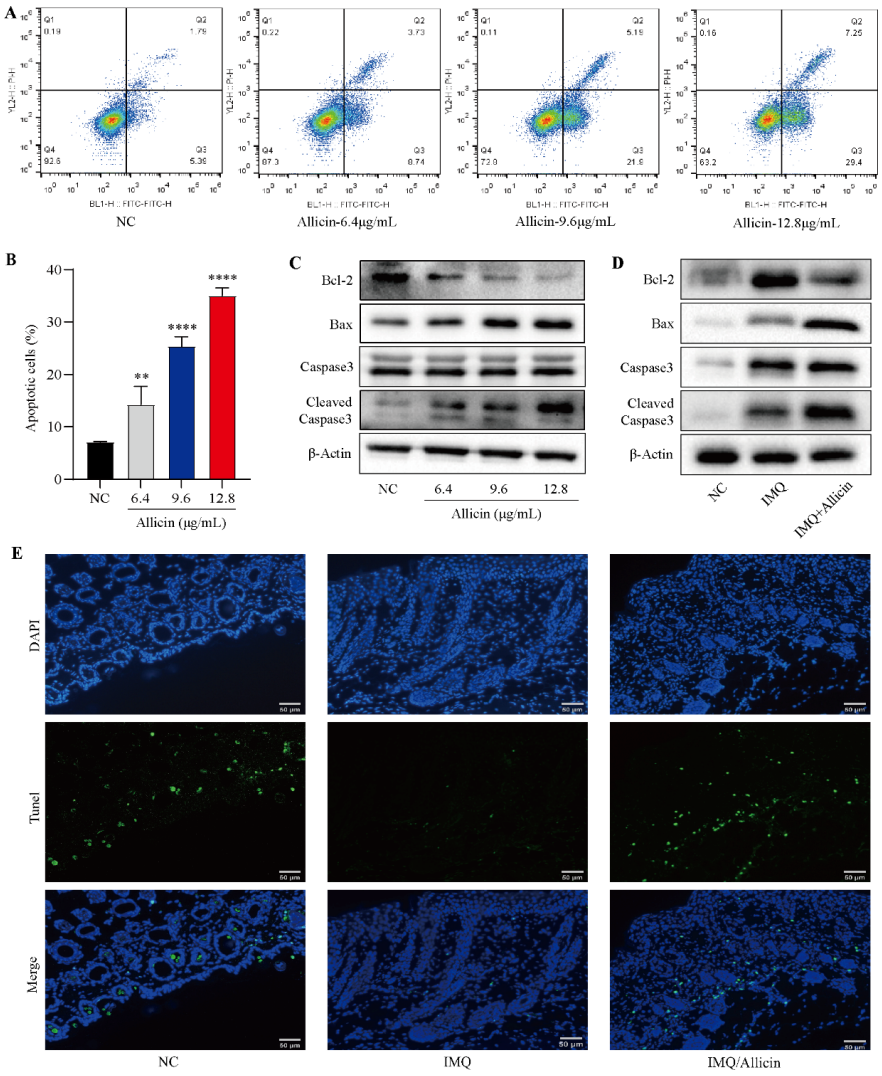

Figure 4. Allicin promotes keratinocytes apoptosis in vivo and vitro. (A) Apoptosis was measured by staining with annexin V/PI staining followed by flow cytometry. (B) Allicin significantly increased the percentage of early apoptotic cells (AV+/PI-) and late apoptotic cells (AV+/PI+) in a dose-dependent manner after 48h (n=3). (C) Western blot analysis of Bax, Bcl-2, and cleaved-caspase3/caspase3 by pretreating the HaCaT cells with different concentrations of allicin for 48 h. (D) Western blot analysis for Bax, Bcl-2, and cleaved-caspase3/caspase3 in IMQ-induced psoriatic lesions with allicin-treated. β-Actin was used as the endogenous loading control. (E) Representative images of skin sections stained with TUNEL (green) to detect apoptotic cells and nuclei were treated with DAPI (blue) in IMQ-induced psoriasis-like lesions treated with or without allicin. Scale bar = 50 μm. Data are expressed means ± SD. *p < 0.05, **p < 0.01, ***p < 0.001, ****p < 0.0001.

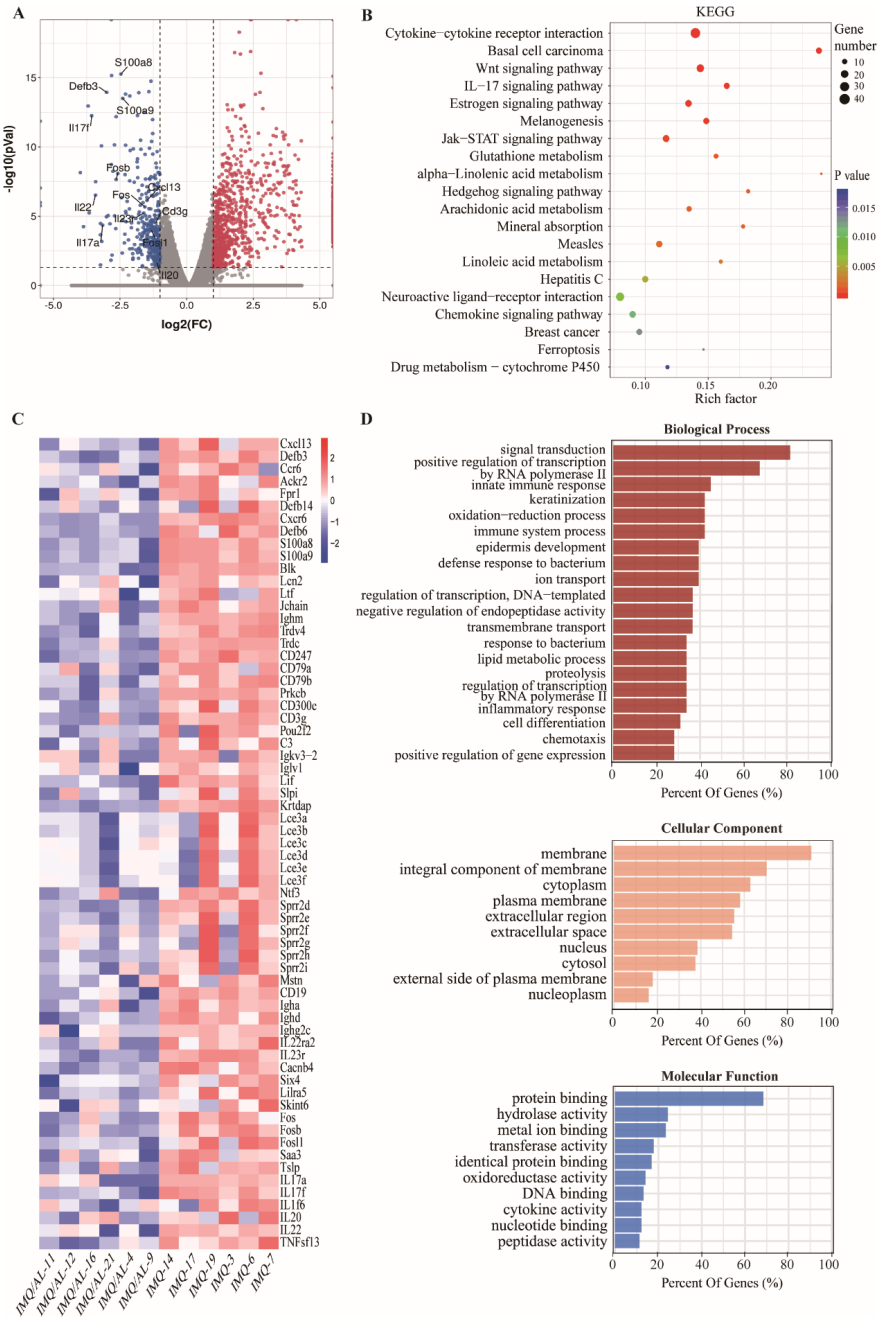

Figure 5. RNA-seq reveals the mechanism of allicin ameliorating IMQ-induced psoriasis-like lesions by repressing the IL-17 signal pathway. (A) Volcano plot of downregulated (blue) and upregulated (red) DEGs between allicin treated/untreated IMQ-induced psoriatic lesions. (B) Heatmap of the top 50 downregulated DEGs with or without allicin. (C) KEGG pathway analysis of DEGs (FDR < 0.1). (D) The downregulated DEGs were classified based on their gene ontology (GO) terms for biological process (BP), cellular component (CC), and molecular function (MF).

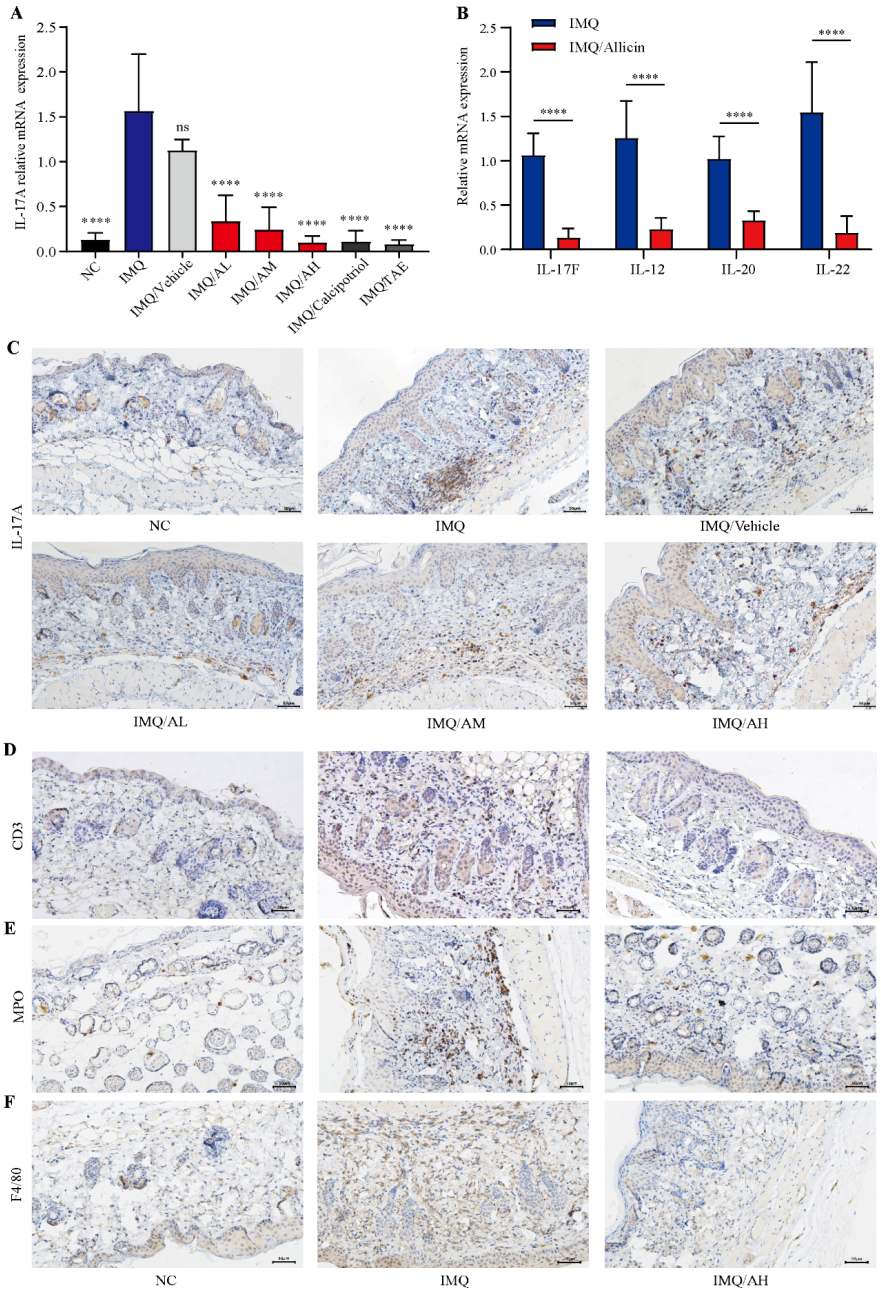

Figure 6. Allicin reduces the overproduction of inflammatory cytokines. (A) Quantitative PCR analysis of mRNA level of the IL-17A genes in back skin treated with IMQ in all groups (n=6). (B) Quantitative PCR analysis of mRNA level of the IL-17F, IL-12, IL-20, and IL-22 genes in IMQ-treated lesions with or without allicin (n=6). (C) Representative immunohistochemical images and the relative expression of IL-17A in each group (AL, allicin low-dose; AM, allicin middle-dose; AH, allicin high-dose; TAE, triamcinolone acetonide and econazole cream). Immunohistochemical staining of CD3+ cells (D), MPO+ cells (E), and F4/80+ cells (F) in IMQ-induced psoriasis-like lesions treated with or without allicin. Scale bar = 50 μm. Data are expressed as means ± SD. *$p < 0.05$, **$p < 0.01$, ***$p < 0.001$, ****$p < 0.0001$.

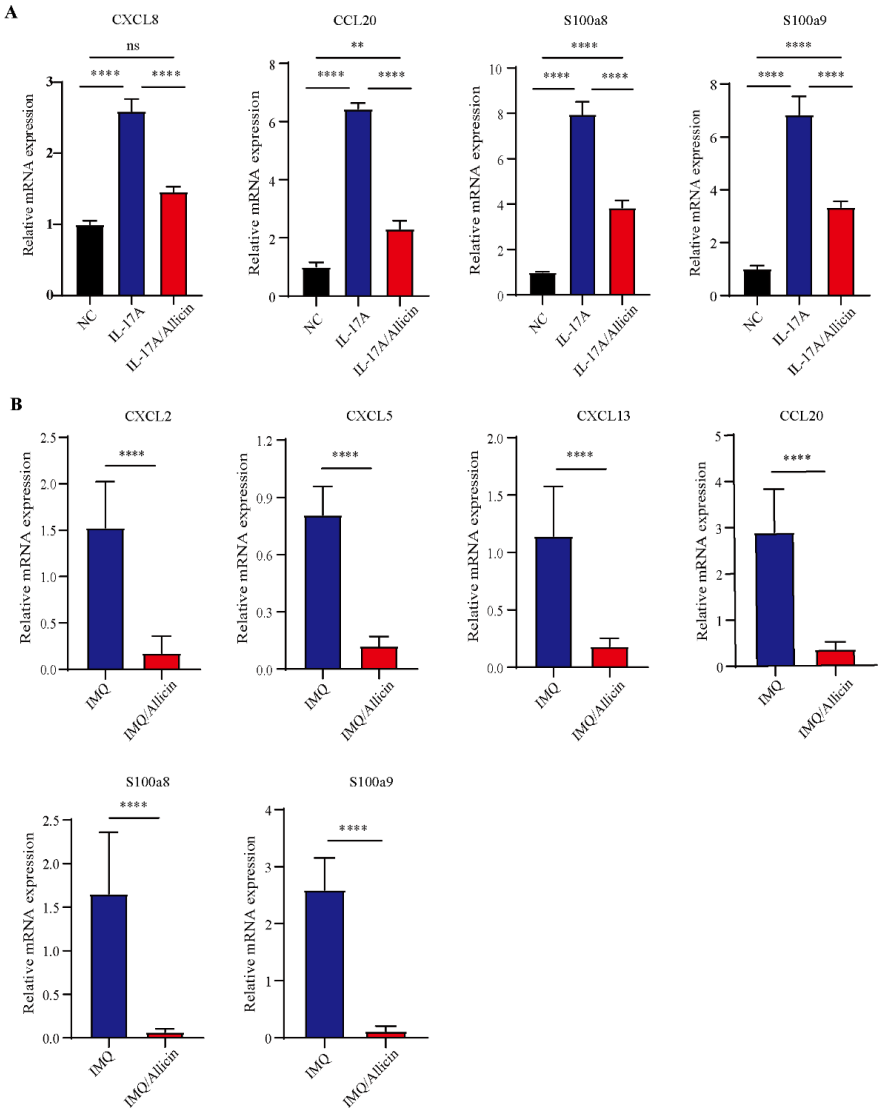

Figure 7. Allicin suppresses the over-expression of chemokines and AMPs. (A) Quantitative PCR analysis of mRNA level of the CXCL8, CCL20, S100a8, and S100a9 genes in IL-17A-stimulated HaCaT cells with or without allicin (n=3). (B) Quantitative PCR analysis of mRNA level of the CXCL2, CXCL5, CCL20, S100a8, and S100a9 genes in IMQ-induced psoriatic lesions treated with or without allicin (n=6). Data are expressed as means ± SD. *$p < 0.05$, **$p < 0.01$, ***$p < 0.001$, ****$p < 0.0001$.

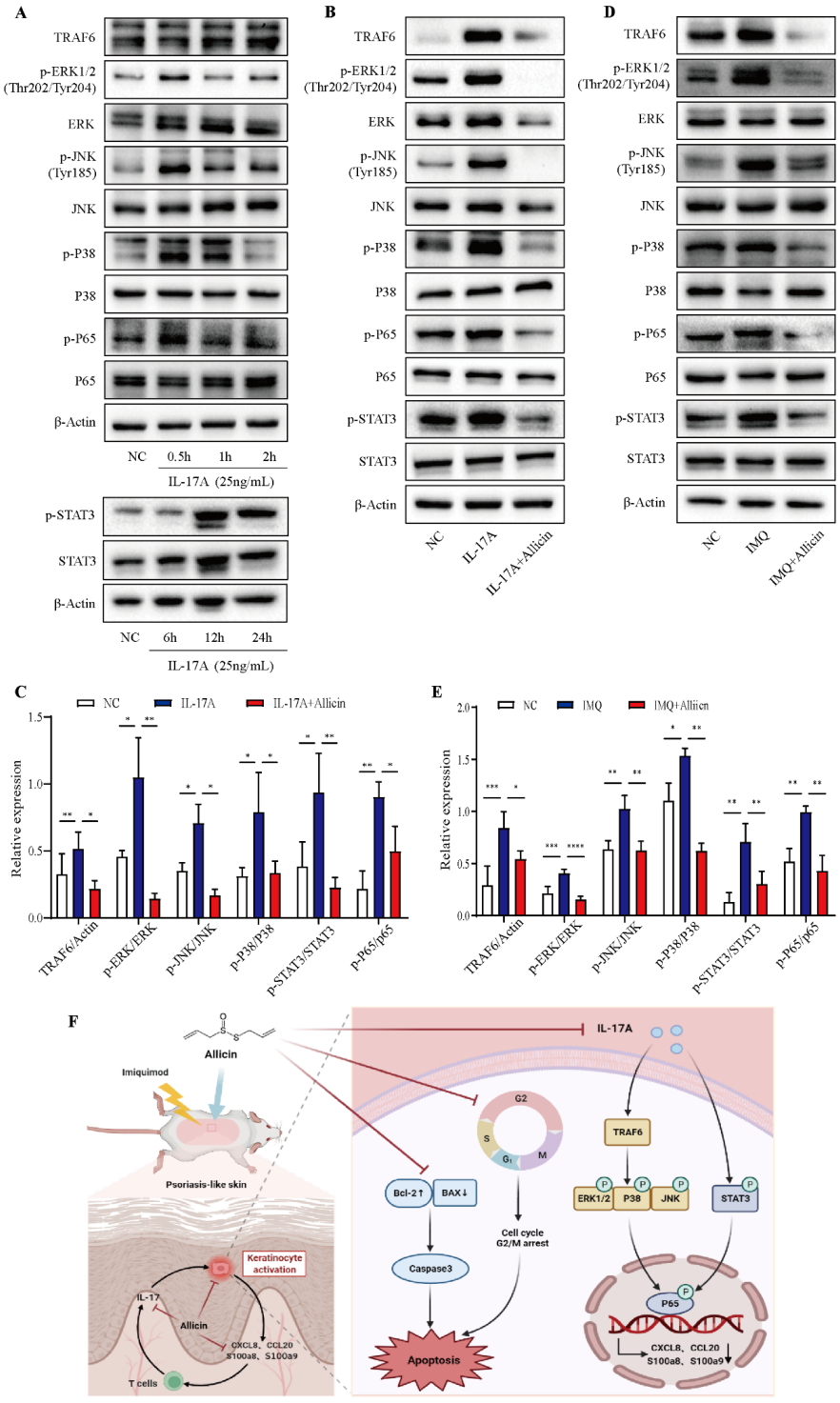

Figure 8. Allicin inhibits the activation of TRAF6/MAPK/NF-κB and STAT3/NF-κB signaling pathways in the IL-17A-stimulated HaCaT cells. (A) The protein expression of TRAF6, p38, phospho-p38, JNK, phospho-JNK, Erk1/2, phospho-Erk1/2, STAT3, phospho-STAT3, p65, and phospho-p65 in HaCaT cells stimulated with IL17A at indicated time points were measured by western blotting. β-actin was used as

a loading control. (B, C) HaCaT cells were pretreated with 12.8ug/ml allicin for 7.5h and subsequently stimulated with IL-17A (25 ng/ml) for an additional 0.5h. Western blot showing the protein expression of TRAF6, P38, phospho-P38, JNK, phospho-JNK, ERK1/2, phospho-ERK1/2, STAT3, phospho-STAT3, P65, and phospho-P65 in HaCaT cells (n=3). (D, E) Western blot showing the protein expression of TRAF6, P38, phospho-P38, JNK, phospho-JNK, ERK1/2, phospho-ERK1/2, STAT3, phospho-STAT3, P65, and phospho-P65 in IMQ-induced psoriasis-like lesions treated with or without allicin (n=5). (F) Putative pathway for allicin-mediated regulation of inflammation and hyperproliferation in IMQ-induced psoriatic lesions. Data are expressed as means ± SD. *$p < 0.05$, **$p < 0.01$, ***$p < 0.001$, ****$p < 0.0001$.